Met. Mater. Int., Vol. 22, No. 3 (2016), pp. 397~406
doi: 10.1007/s12540-016-5495-x

Effect of Punch Speed on the Formability Behavior of Austenitic Stainless Steel Type 304L

H. Fathi[1], E. Emadoddin[1,*], H. R. Mohammadian Semnani[1], and B. Mohammad Sadeghi[2]

[1]Faculty of Materials and Metallurgical Engineering, Semnan University, Semnan, Iran
[2]Faculty of Metallurgy and Materials Engineering, Iran University of Science and Technology, Iran

(received date: 10 September 2015 / accepted date: 8 January 2016)

The aim of the present study is to investigate the effect of punch speed on forming limit diagram (FLD) and the formability of austenitic stainless steel type 304L. Effect of strain rate on the height of dome is studied using the hemispherical punch test. Results of this study show that strain rate has significant effect on FLD in this material and high formability obtains at low strain rate. The safe area of FLD between major and minor strains is extended under low strain rate. It is seen that at low punch speed, failure and fracture occur at the pole region (top of the dome), whereas at higher forming rates, failure occurs close to the flange region. Modeling studies are also carried out using Ls-Dyna to know the region of high stress concentration and to predict the location of fracture. There is good agreement between simulation and experimental results.

Keywords: metals, deformation, strain rate, computer simulation, forming limit diagram

1. INTRODUCTION

Stainless steels have been used in variety of applications in construction and other industries due to material advantages that include a unique combination of weld-ability, strength, corrosion resistance and toughness [1,2]. These types of steels are suitable for use under condition of high temperatures [3]. Recently, there has been much focus on the application of stainless steels in fabrication of crash resistance structural parts in automotive industries due to the high energy absorption of these materials, along with good formability that is very important [4]. Martensitic transformation in austenitic stainless steels plays an important role on their formability. Indeed, martensitic transformation in stainless steel is a phenomenon that is controlled by nucleation [5]. The kinetic of transformation in austenitic stainless steel depends upon many parameters such as stress state, strain, strain rate and temperature [6,7]. Austenite phase is a preferential phase because it can provide both strength and ductility in sheet metal forming. Martensitic transformation in austenitic stainless steel enhances the ability of work hardening behavior. Then, it postpones the localized necking and improves the formability of sheets and transformation occurs via the mechanism of transformation induced plasticity [8,9]. Transformation rate may be controlled by the stability of austenite phase and thus the mechanical properties of the material can be affected through it. In the meantime, factors such as enrichment of carbon, chemical composition and austenite grain size also have significant effects on the stability of austenite phase [7].

FLD represents the major strain without any fracture in the blanks of metals. In the other hands, maximum strain before fracture in the process of sheet metal forming may be obtained by FLDs [10]. FLD is thus a very useful concept to define the formability of sheet metals. FLD concept was proposed by Keeler, Backofen and Goodwin, in 1964 and 1968 [11,12]. FLDs are usually determined in two well-known ways. The first is to use the Marciniak test (Hole Expansion Test), which leads to frictionless deformation. The second is to utilize the Nakazima test (hemispherical dome test) which is widely using in scientific studies and yields more reproducible results than the Erichsen cup tests [13]. It is proved that the deeper dome shows better formability of the sheet metals [14]. The most important parameters that affect the behavior of FLDs are lubrication, thickness of sheet metal, preferred orientation of grains and material properties [15].

Many authors have studied martensitic transformation in some types of austenitic stainless steels. It should be pointed that many of these investigations have focused on tension, compression properties and deep drawing test [5,16-19], but there are not many comprehensive reports on the effect of strain rate on FLD for stainless steel type 304L. There is a need for better understanding the effect of transformation on the formability of stainless steel sheets. This paper presents the result of an extensive investigation on the effect of martensitic transformation on the behavior of FLD for austenitic

*Corresponding author: emadoddin@semnan.ac.ir

stainless steel type 304L to identify the FLD curve and fracture location in the stretch forming process.

Recently, there have been many attempts at simulation using ABQUSE and LS-DYNA software to validate the experimental result in all scientific fields. Simulation studies can be useful for understanding the formability behavior of sheet metals before performing experiments. In the present work, the formability of stainless steel type 304L was studied by determining FLDs of the material at three various forming speed. Experimental tests were then performed to compare and verify the simulation results obtained from Ls-Dyna using MAT_TRIP. The regions with high stress concentration and fracture area in the samples were simulated by the software.

2. EXPERIMENTAL PROCEDURE

2.1. Material preparation

In this study, austenitic stainless steel type 304L sheet with thickness of 0.5 mm was used in the experiments. Chemical composition of the origin material is represented in Table 1. Based on the ASTM E8, three samples with 30 mm gage length were used for the uniaxial tension test using 40ton hydraulic press under three various punch speeds of 3, 30 and 300 mm/min for understanding the effect of martensitic transformation on the mechanical properties of the sheet. Increasing of the sample temperature during tensile test at the gage length portion was measured by accurate K-type thermocouple, which was attached to the gage length of the sample.

The sheet metal was then cut to samples using cutter for dome test. Eight samples were used for each test to construct a FLD curve. Rectangular blanks were cut to different widths ranging from 25 mm to 200 mm in increments of 25 mm. All blanks were cut in the same direction in the width from the initial material. They were provided along the rolling direction of the sheet product [20]. Test samples are shown in Fig. 1.

Grid patterns of square, circle, dot or combination of them are using to measure minor and major strains for determining FLD curves. Preferred shape and size of the grid consist of a circle with 2.5 mm diameter [20,21]. It is noted that using grids with larger diameter leads to obtain uncertain results. Chemical etching equipment photo grids was used to produce circle grid pattern on the samples surface as shown in Fig. 2(a).

The minor and major strains were measured using a Mylar transparent tape. The Mylar tape was drawn by Solidworks software and then printed on a transparent sheet. Diameters from 1 mm to 7 mm could be measured using this tape. For calculating the minor and major strains after dome test, the Mylar tape was fitted on the grids and photographed using a high resolution camera to measure maximum and minimum diameter of the grids as shown in Fig. 2(b).

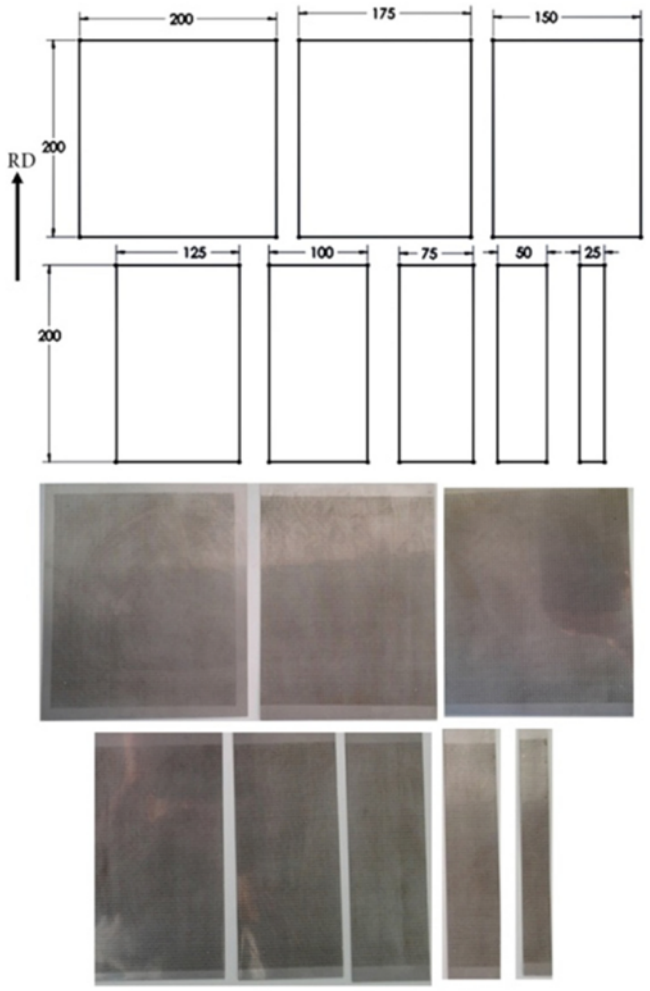

Fig. 1. Rectangular strips with various widths ranging from 25 mm up to 200 mm.

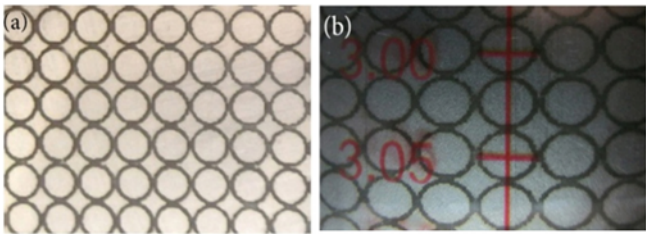

Fig. 2. (a) Circle grid patterns on the samples surface and (b) measuring the major and minor diameter of ellipsoid after straining by Mylar tape technique.

2.2. Test instruments

A forming die having 75 mm punch diameter was manu-

Table 1. Chemical composition of the origin material (wt%)

Fe	C	Si	Mn	S	P	Cr	Ni	Co	V	Remain
Base	0.026	0.55	1.07	0.001	0.029	18.38	8.18	0.37	0.112	Other elements

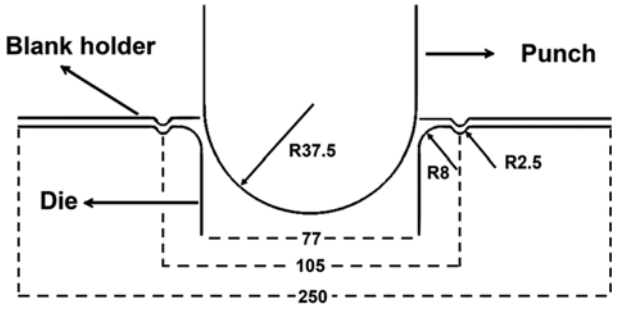

Fig. 3. Die and punch dimensions (unit: mm).

factured to perform dome test with 40ton hydraulic press. The plan of the die and punch used in the experiments are shown in Fig. 3. A pair of grooves with diameter of 2.5 mm was designated in both die and blank holder to grip the blank between die and blank holder. In all cases such as deep drawing and dome test, lubricant must be used to decrease the effect of friction between punch and blank. Here, a Teflon sheet was applied between punch and blank to reach minimum friction coefficient.

Eight tests should be performed to obtain each FLD curve. The blank was placed between the die and blank holder and the press was made to move through the die. When necking occurred in the formed cup, the press load was decreased and the machine was stopped. Figure 4 shows blanks that were tested at various punch speeds of 3, 30 and 300 mm/min. As can be seen in the Fig. 4, the fracture behavior of the samples with various punch speeds is very different. It is clear that fracture in the blanks that were tested with punch speed of 3 mm/min occurred at the top of the dome, whereas in the samples tested at the higher punch velocity, fracture occurred in the middle of cup height.

Table 2. Tests parameters

Num	Punch speed (mm/min)
1	3
2	30
3	300

The parameters that were investigated in this research are summarized in Table 2. As presented in Table 2, three values of punch velocity were tested to draw FLD and volume fractions of transformed martensite during stretching were compared. The effect of martensitic transformation on FLD behavior was studied.

3. SIMULATION

Simulations of experiments were done using *MAT_TRIP in Ls-Dyna 971. Transformation rate can be achieved using TRIP material model. Hardening behavior by yield stress is described according to Eq. 1 for TRIP material in Ls-Dyna [22]:

$$\sigma_y=\{B_{Hs}-(B_{HS}-A_{HS})\exp(-m[\bar{\varepsilon}^p+\varepsilon_0]^n)\}(K1+K2T)+\Delta H_{\gamma\to\acute{\alpha}}Vm \quad (1)$$

where:

$\bar{\varepsilon}^p$: Effective plastic strain,
T: initial temperature
K1, K2, m, n, $\Delta H_{\gamma\to\acute{\alpha}}$: Martensite rate equation parameters

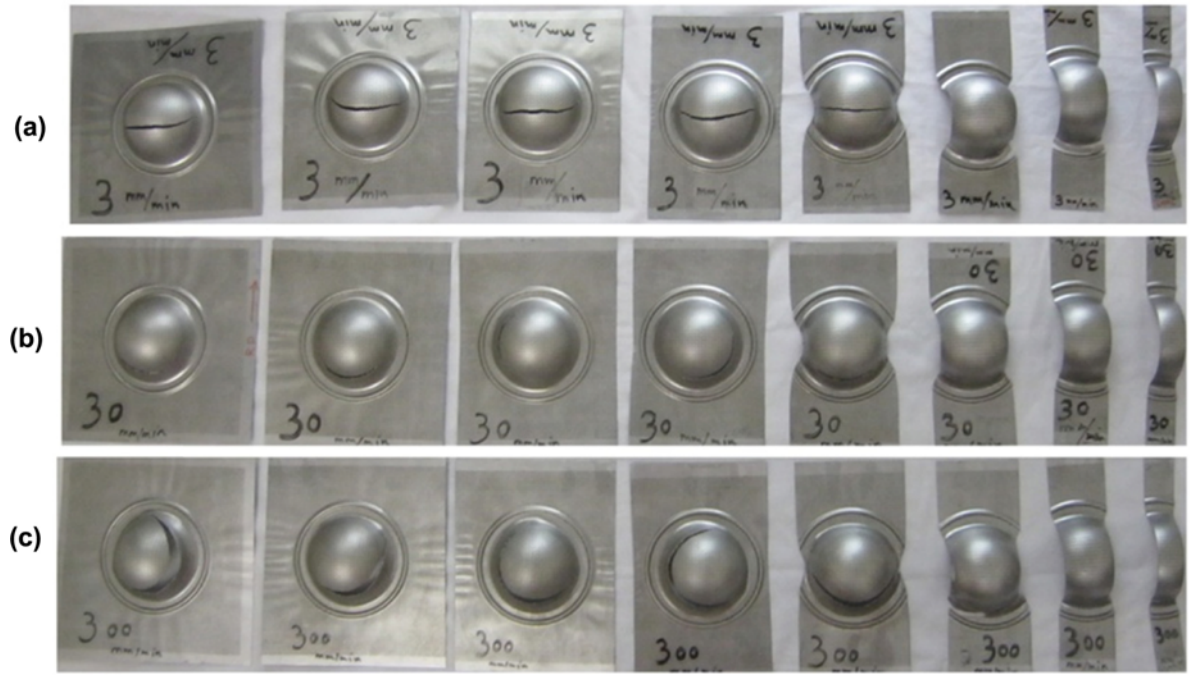

Fig. 4. Dome formation and fracture location in the blanks were tested with punch speeds of 3 (a), 30 (b) and 300 mm/min (c).

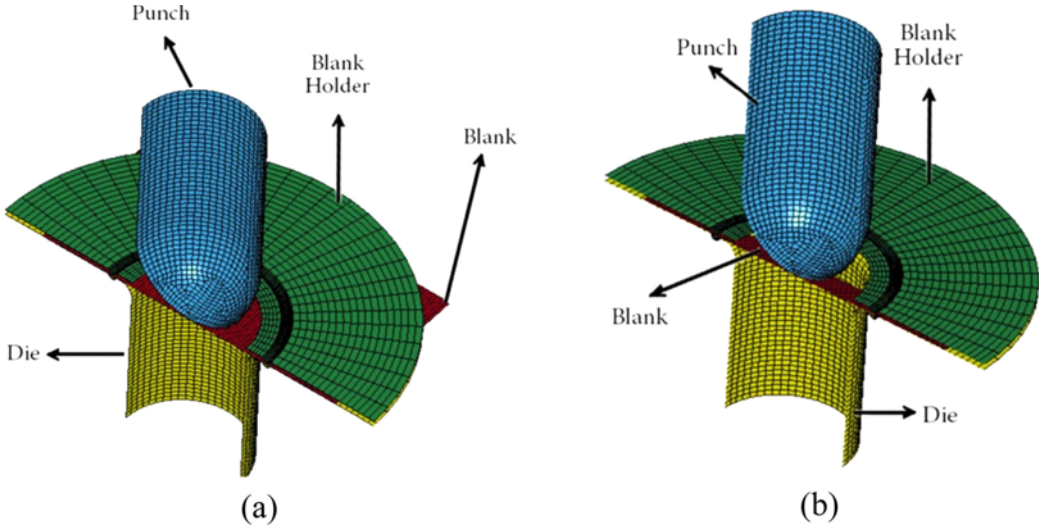

Fig. 5. Modeling of the dome test for (a) the rectangular blanks with 200 mm width and (b) the strip blanks with 25 mm width.

ε_0: Pre-strain
A_{HS}, B_{HS}: Hardening law parameters
V_{m0}: Initial volume fraction of martensite

In austenitic stainless steels, martensitic transformation affects the yield stress but does not affect the ultimate strength [23]. For this reason, yield stress of the material may change during the forming process. Yield stress of the material should be calculated to take into account the updated yield stress during calculation by the software. In the other words, yield stress that changes during deformation is calculated by Eq. 1. 3D modeling of dome test was carried out in the Ls-Dyna using shell element as shown in Fig. 5.

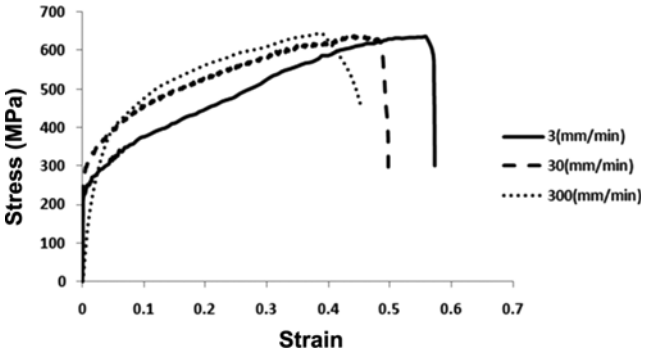

Fig. 6. Stress-strain curves for the sheet tested at three punch speeds.

4. RESULTS AND DISCUSSION

4.1. Material behavior under uniaxial tensile test

As previously mentioned, austenitic stainless steel type 304L shows different behaviors under various strain rates. Engineering stress-strain curves for the sheet tested with three punch speeds (three strain rates) are shown in Fig. 6. It can be understood from the figure that flow stress increases with increase in strain rate. It reveals that there is an increase in yield stress with increase the strain rate, while ultimate tensile stress is not affected by the strain rate and remains constant about 640 Mpa under all punch speeds. It is noted that the fracture strains are about 0.56 and 0.39 when punch speeds are 3 (low strain rate) and 300 mm/min (high strain rate), respectively. The ultimate tensile stress of austenitic stainless steel type 304L is insensitive to strain rate until high value of strain rate [23,24]. Using magnetic saturation method showed that about 33% and 19% of martensite were formed in tensile test samples tested under punch speeds of 3 and 300 mm/min, respectively. As the result, more martensitic transformation leads to increase work hardening under low strain rate and failure occurs at the high strain (0.56). While, high strain rate restrains martensitic transformation and reduces work hardening, consequently failure occurs at the low strain (0.39).

The sample temperature rise measured during tensile test is shown in Fig. 7. It shows that temperature of the gage length increases with increase the strain rate. Indeed, shear band intersection decreases through strain rate adiabatic thermal due to increase in temperature at high strain rate condition. Since, martensite nucleates at the shear bands intersection, therefore martensitic transformation increases with decrease the strain rate [5,6,16,25]. According to Fig. 6 and Fig. 7, as the punch speed (strain rate) decreased, temperature of the sample decreased, therefore higher elongation obtained by more martensite volume fraction.

4.2. Height of dome

In the method of determining FLD for sheet metals, identification of conditions that can result in maximum height of dome is very important. Here, important parameters that have significant effects on the sheet formability were found and then the optimum parameters were applied to the test process.

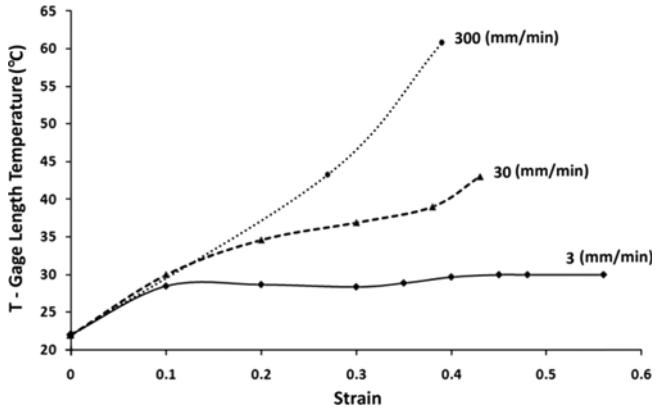

Fig. 7. Temperature rise under stroke velocity of 3, 30, and 300 mm/min during tensile test.

As mentioned, Teflon sheet was used between punch and blank to reduce the effect of friction. Frictional shear stress causes failure and limits the height of dome. Strain rate is the other important parameter that was applied in the test process. Figure 8 shows the maximum height of dome under different punch travel velocities.

Generally, dome test indicates that samples with higher dome height have more ductility and formability. From Fig. 8 and Fig. 9, it can be found that the highest height of dome can be achieved by applying the lowest punch speed. The main reason for this observation is that high strain rate causes reduction of martensite transformation from austenite [17]; this results in a fall in the hardening capacity that leads to easier and faster necking and failure.

As seen in Fig. 9, a higher forming load is required to obtain a higher dome. For instance, for the blank that was tested with punch speed of 3 mm/min, about 79000N force is needed to obtain 42.26 mm height of dome, while in the blank tested with punch speeds of 30 and 300 mm/min, about 70000N and 58000N force are required to form domes with the heights of 36 and 33.37 mm, respectively. It can be noted that lower strain rate is needed to get more uniform elongation. Furthermore, more transformation may have occurred at low strain rates. This means that for this material at low strain rate, higher forming force is needed to obtain higher height of dome.

4.3. Determination of FLD Curve

As mentioned in Fig. 4, there are three groups of blanks that in each group there are eight blanks. Experiments were conducted on the strip sheets from 25 mm to rectangular blank with 200 mm width. Dome test on each group of the blanks were performed with punch speeds of 3, 30 and 300 mm/min to investigate the effect of the strain rate on transformation and FLD curve behavior, Fig. 10.

As can be understood from Fig. 10, FLD with punch speed of 3 mm/min, which is the lowest velocity in this work, is much higher than the others. It means that higher depth of the dome obtains at low strain rate and low strain rate enhances the

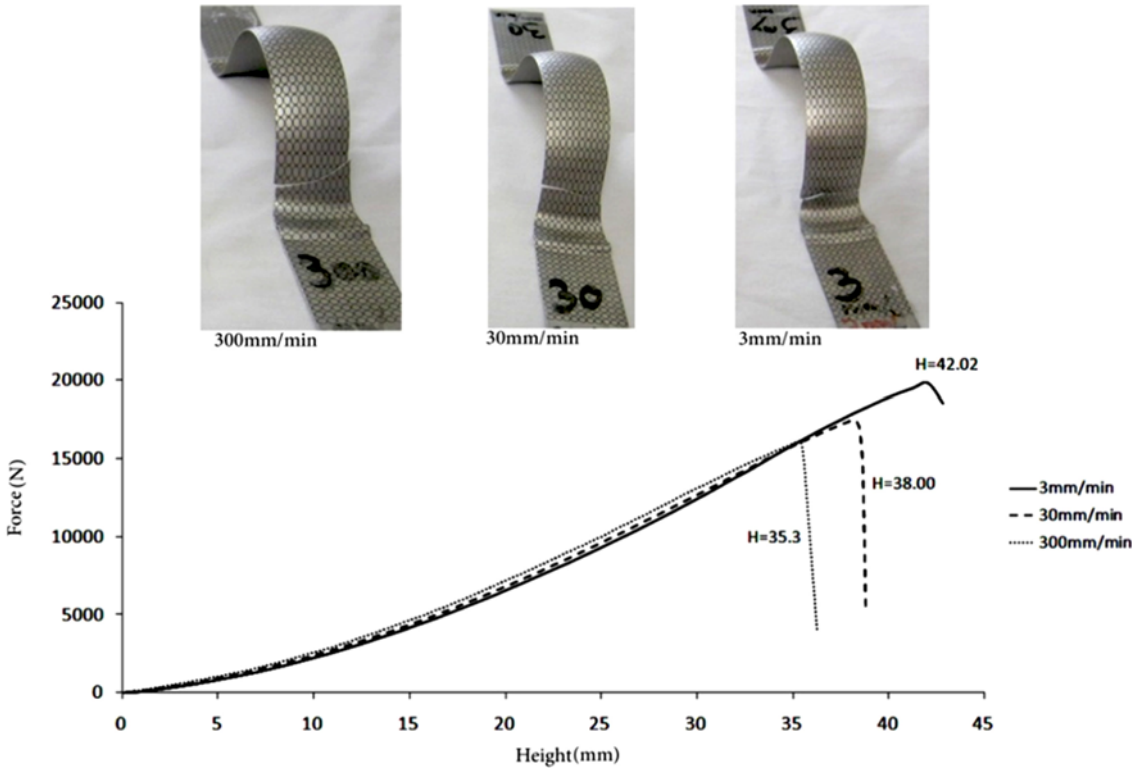

Fig. 8. Force-height of dome plot for the strip sample with 25 mm width was stretched by different punch speeds.

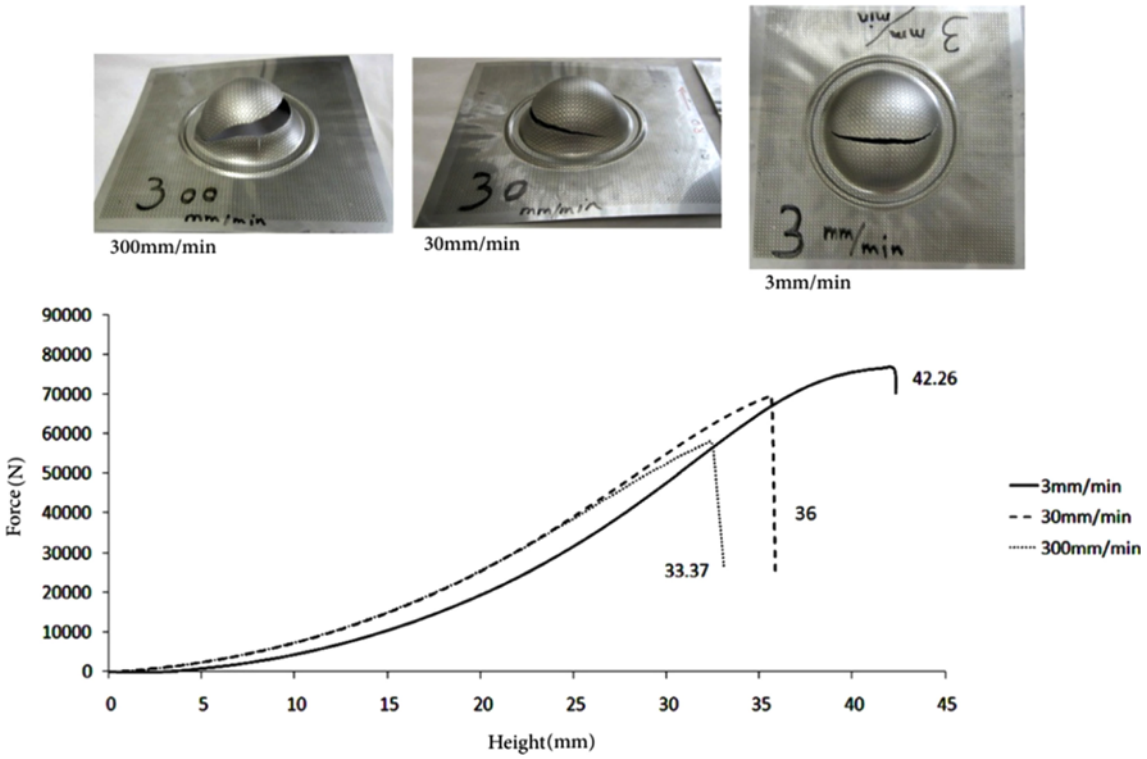

Fig. 9. Height of dome curve for the rectangular samples with 200 mm width for three punch speeds.

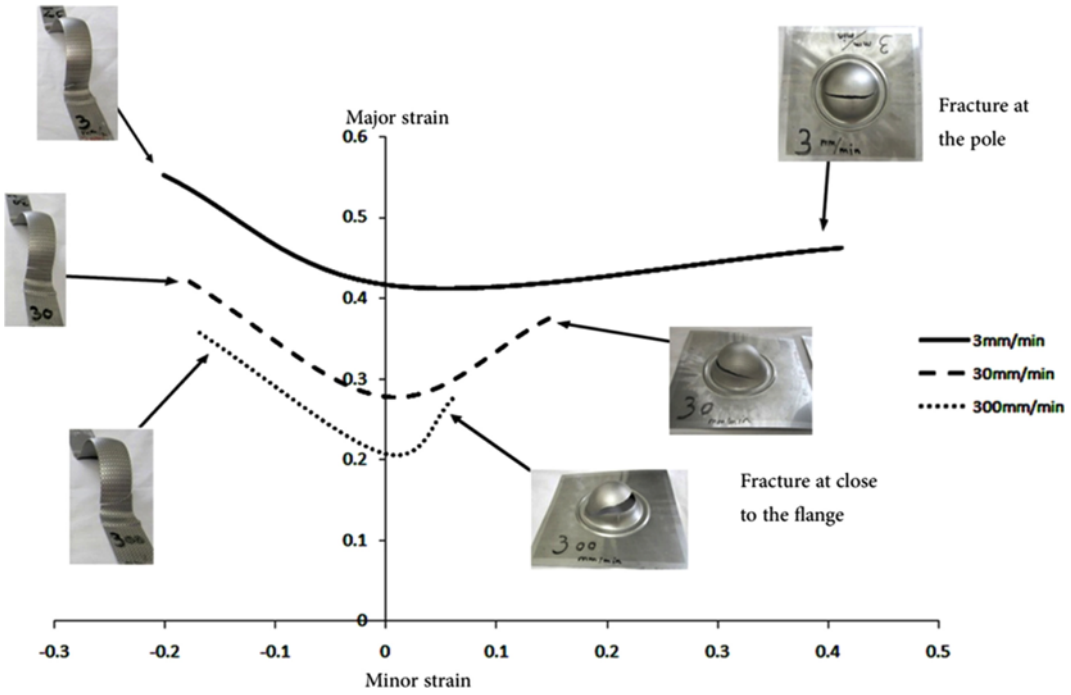

Fig. 10. Comparing FLD curves of tested materials at different punch speeds.

formability of the blanks. Figs. 11(a) and 11(b) represent the maximum strain regions for the rectangular blanks at the lowest and highest strain rates and Figs. 11(c) and 11(d) show the maximum strain regions for the strip sheets at the lowest and highest strain rates, respectively. Results show that failure locations seen during experiments agree with the predicted failure loci in simulation; thus there is good agreement between experiment and simulation. In both experiments and simulations, it is observed that for punch speed of 3 mm/min maximum strain occurs at the pole, whereas with punch speed of

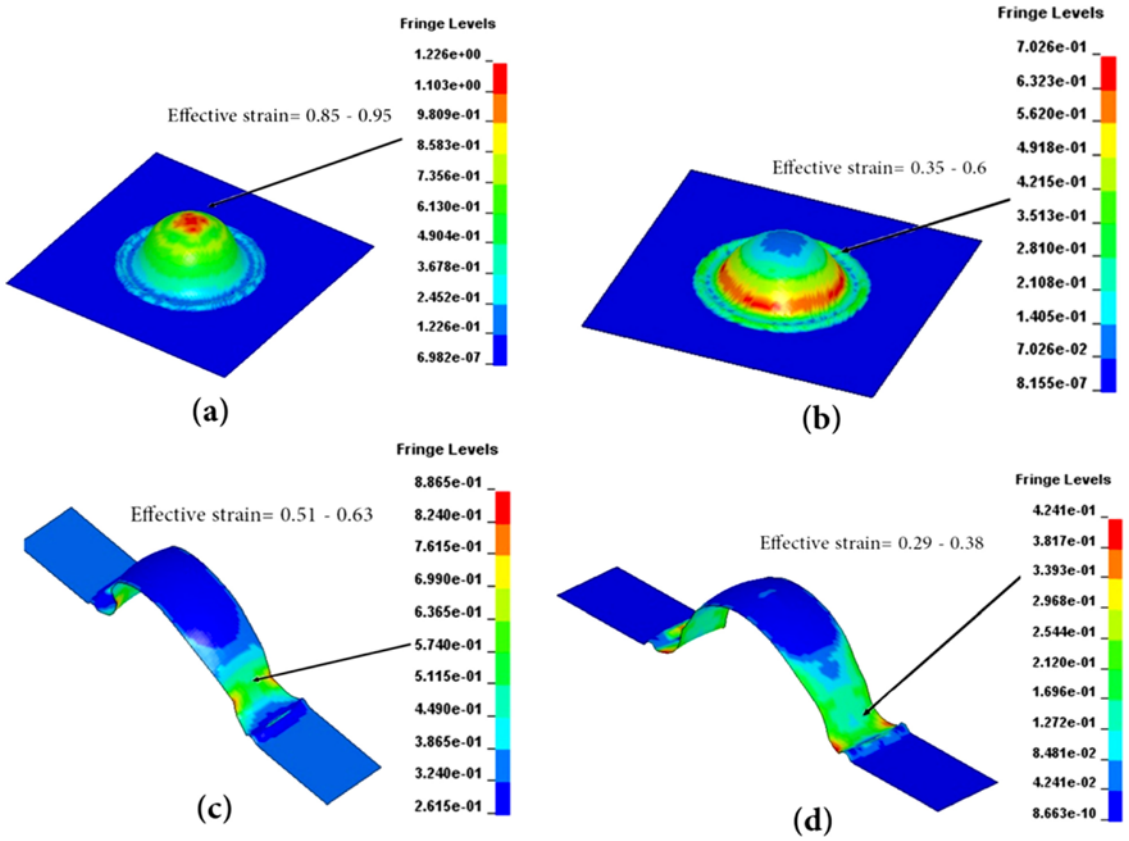

Fig. 11. Maximum strain region by simulation in stretched samples with 200 mm width for punch speed of (a) 3, (b) 300 mm/min and in samples with 25 mm width for punch speed of (c) 3, (d) 300 mm/min.

Table 3. Effective strains of stretched samples by experimental and simulation

Sample size (mm)	Punch speed (mm/min)	Effective strain (Experimental)	Effective strain (Simulation)
200×200	3	0.879	0.85-0.95
	300	0.44	0.35-0.6
200×25	3	0.565	0.51-0.63
	300	0.354	0.29-0.38

300 mm/min maximum strain occurs close to the flange region.

Figure 10 shows that the critical region is between strains of 0.46 (minor strain) to 0.415 (major strain) at the lowest strain rate (punch speed of 3 mm/min) but measured strain at higher strain rates is between 0.146 (minor strain) to 0.277 (major strain) and the critical strains at the highest strain rate (punch speed of 300mm/min) are about 0.0631 (minor strain) to 0.206 (major strain). Increasing the strain rate causes decrease in critical strain range, which is very important in the forming process. Therefore, according to these results, in the forming process of stainless steel 304L, to achieve the highest proposed strain, it should be stretched under lower strain rate to obtain the highest formability of the blanks.

Figure 11 shows the critical region with maximum strain during the forming process. Effective strain of the samples with a width of 200 and 25 mm for punch speeds of 3 and 300 mm/min, compared with simulation results are represented in Table 3. Based on Table 3 and Fig. 11, it is clear that simulation results show good agreement with experimental results in terms of fracture location and effective strain with the experiments.

Main factors that have significant effects on martensitic transformation in austenitic stainless steel are strain rate, temperature, plasticity and stress state. Strain rate is one of the most important factors that it decreases shear band intersections because of strain rate adiabatic heating [17,25]. Increase in the strain rate causes increase in the temperature. Strain rate and temperature rise lead to reduce martensitic transformation during forming process. It is pointed that shear bands formation with the increasing strain rate controls deformation mode. On the other word, the shear bands decrease when the temperature of the sample is higher [25].

It should be mentioned that increasing the strain rate causes an increase in the temperature at the certain strain. The strain rate reduces the time for decreasing total of heat flow loss

and then rises temperature of the sample. Decreasing the strain rate increases martensitic transformation at the specific strain, consequently it increases volume fraction of martensite. It is notable that creation of shear bands is reduced when there is an increase in temperature [5]. In the initial stage of deformation, generation of shear bands is fast but it is reduced with decreasing the consumption of shear bands [26]; therefore increasing the strain rate rises temperature and reduces shear band generation rate. The outcome of this phenomenon is low volume fraction of martensite. Furthermore, it should be considered that increasing the temperature leads to decrease chemical driving force; hence, higher strain rate causes lower martensitic transformation [5]. For these reasons, samples that were tested at lower strain rate show the highest dome height; in contrast, the samples formed with higher strain rate have the lowest dome height.

Considering FLD under various punch velocities, it is clear that at low strain rate, FLD shifts to the right and at higher strain rates FLD shifts to the left. It means that fracture occurs at the pole and FLD tends to equi-biaxial strain state condition under lower strain rate. In contrast, at higher strain rates fracture occurs close to the flange and the FLD tends to uniaxial strain state.

4.4. Fracture behavior

As mentioned above, fracture occurs in various locations with different strain rates during dome test. Blanks that were tested with low forming speed fractured at the pole of the dome, while fracture happened at the middle of the dome (close to the flange) with high punch speeds. Figures 11(a), 11(b) and 11(c) show the fracture locations for rectangular blanks with various widths from 100 mm up to 200 mm with punch speeds of 3, 30 and 300 mm/min, respectively. Furthermore, strip blanks with width of the range of 25 mm to 75 mm with punch speeds of 3, 30 and 300 mm/min, are shown in Figs. 12(a), 12(b), and 12(c), respectively. Since, the fracture behaviors are different at various punch velocities, so the strips are divided into separate figures.

As shown in Fig. 12, in the blanks that were tested with punch speed of 3 mm/min failure occurred at the pole of the dome with the highest height of dome, while with punch speeds of 30 and 300 mm/min failure occurred close to the flange with low height of the dome. It should be mentioned that hardening due to strain induced phase transformation is the main phenomenon that affects the ductility improvement. Martensitic transformation causes more martensite volume fraction and then uniform elongation enhances at low strain rate [5,27]. This means that ductility is enhanced at low strain rate and failure delayed until higher ductility and uniform elongation are obtained at the pole of the dome. Magnetic saturation test was conducted to measure volume fraction of martensite that was transformed from austenite in the samples at various strain rates. Maximum volume fraction of martensite about 56% at the pole and 46% close to the flange were

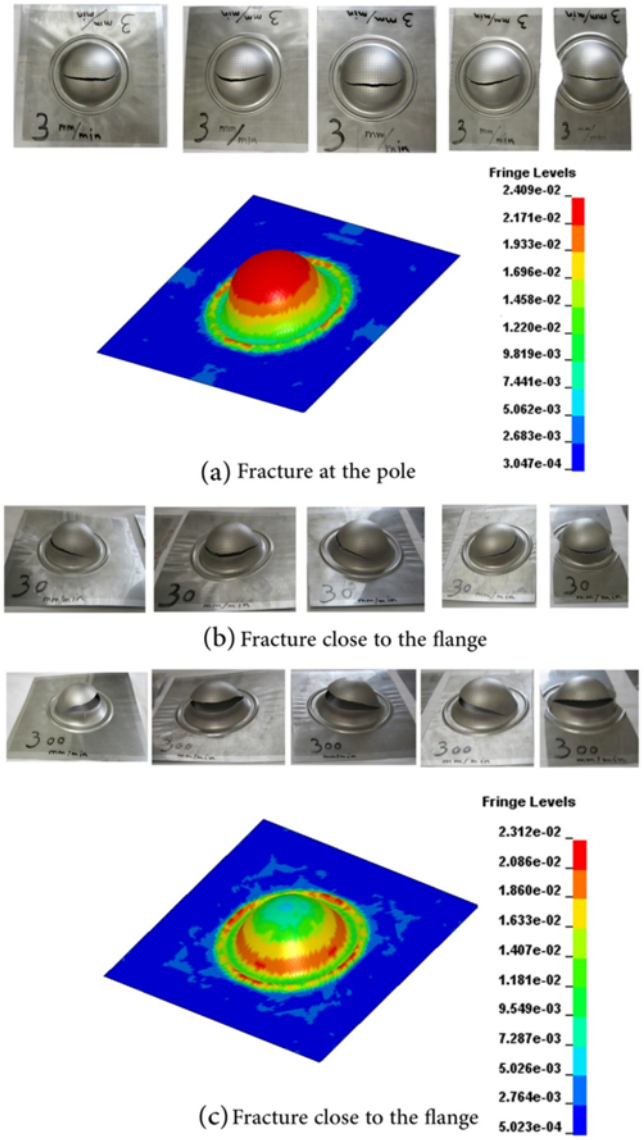

Fig. 12. Fracture location (up) and effective equivalent stress by simulation ($\times 10^4$ MPa) (down) at forming punch speeds of (a) 3 mm/min, (b) 30 mm/min, and (c) 300 mm/min for blank sizes from 100 mm to 200 mm.

obtained with punch speeds of 3 and 300 mm/min, respectively. Results show that maximum volume fraction of martensite is formed at low strain rate and elongation enhanced. According to the simulation results, it can be seen that at low strain rate, critical effective stress occurs at the pole region but under high strain rate, it occurs close to the flange region. These findings show the good agreement between experimental and simulation results.

As can be seen in Fig. 13, in the strips with a width of 25 mm to 75 mm failure occurs close to the flange region. More martensitic transformation forms under biaxial tension rather than uniaxial tension and the highest volume fraction of martensite forms under triaxial tension stress [28]. Further-

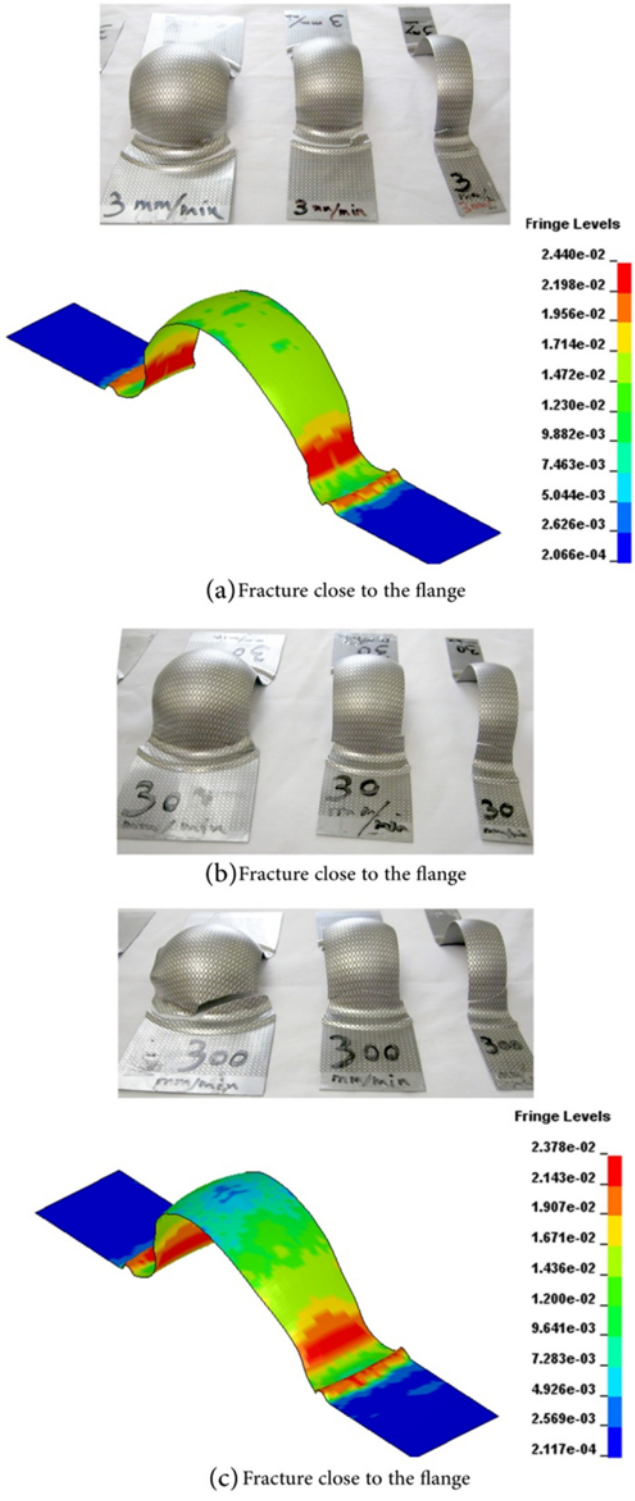

Fig. 13. Fracture location (up) and effective equivalent stress by simulation ($\times 10^4$ MPa) (down) on samples have been stretched with punch speeds of (a) 3 mm/min, (b) 30 mm/min, and (c) 300 mm/min for blanks widths of 25 mm to 75 mm.

more, various strain states in different regions lead to change in volume fraction of martensite because of various states of stress conditions [28]. For this reason, in all strips with width from 25 up to 75 mm with punch speeds of 3 mm/min, 30 mm/min and 300 mm/min, failure occurred close to the flange region, because the state of stress at the pole and close to the flange are different and this condition causes different strains as mentioned in Fig. 11 and Table 3. The simulation results are validated by experiment evidences.

5. CONCLUSION

The purpose of this study is to investigate the effect of forming punch speed on FLD and height of dome in stainless steel type 304L. Dome test was performed under three punch speeds of 3, 30 and 300 mm/min to study the changes in FLD at different strain rates. Results show that at low strain rate, the height of the dome is high and decreases with higher strain rates. Strain rate thus affects FLD and much safety area in FLD obtains under low strain rate. More martensitic transformation may occur at lower strain rate and this phenomenon can delay localized necking and failure in the samples. Thus, martensitic transformation enhances formability of the sheet. Dome test was also simulated by Ls-Dyna and utilizing MAT_TRIP. It is noted that experimental evidences on fracture loci are in good agreement with simulation results.

REFERENCES

1. Y. Kasuga, T. S. Park, I. K. Park, and C. Miyasaka, *Met. Mater. Int.* **18**, 265 (2012).
2. X. P. Ma, L. J. Wang, C. M. Liu, and S. V. Subramanian, *Mater. Sci. Eng. A* **539**, 271 (2012).
3. L. Gardner, A. Insausti, K.T. Ng, M. Ashraf, *J. Constructional. Steel. Res.* **66**, 634 (2010).
4. J. A. Lichtenfeld, M. C. Mataya, C. J. V. Tyne, *Metall. Mater. Tran. A* **37**, 147 (2006).
5. H. N. Han, C. G. Lee, D. W. Suh, S. J. Kim, *Mater. Sci. Eng. A* **485**, 224 (2008).
6. A. M. Beese and D. Mohr, *Acta. Mater.* **59**, 2589 (2011).
7. T. K. Shan, S. H. Li, W. G. Zhang, Z. G. Xu, *Mater. Des.* **29**, 1810 (2008).
8. J. A. R. Martinez, R. Pesci, A. Rusinek, *Mater. Sci. Eng. A* **528**, 5974 (2011).
9. R. Ueji, Y. Takagi, N. Tsuchida, K. Shinagawa, Y. Tanaka, T. Mizuguchi, *Mater. Sci. Eng. A* **576**, 14 (2013).
10. S. M. Hussaini, G. Krishna, A. K. Gupta, S. K. Singh, *J. Manuf. Processes*. **18**, 151 (2015).
11. R. Makkouk, N. Bourgeois, J. Serri, B. Bolle, M. Martiny, M. Teaca, and G. Ferron, *Eur. J. Mech. A-Solids.* **27**, 181 (2008).
12. R. Safdarian, R. M. N. Jorge, A. D. Santos, H. M. Naeini, M. P. L. Parente, *Int. J. Mater. Form.* **8**, 293 (2015).
13. ASM Metal Handbook, *Forming and Forging*, Vol.14, pp. 1962-1963, ASM international, USA (1996).
14. M. Safaeirad, M. R. Toroghinejad, and F. Ashrafizadeh, *J. Mater. Process. Technol.* **196**, 205 (2008).

15. F. Djavanroodi and A. *Derogar, Mater. Des.* **31**, 4866 (2010).
16. X. Li, J. Chen, L. Ye, W. Ding, and P. Song, *Acta Metall. Sin. (Engl. Lett.)* **26**, 657 (2013).
17. P. Hedstrom, L. E. Lindgren, J. Almer, U. Lienert, J. Bernier, M. Terner, and M. Oden, *Metall. Mater. Tran. A* **48**, 1039 (2009).
18. M. Isakov, S. Hiermaier, and V. T. Kuokkala, *Metall. Mater. Tran. A* **46A**, 2352 (2015).
19. E. S. Perdahcıoglu and H. J. M. Geijselaers, *Acta Mater.* **60**, 4409 (2012).
20. ASTM E2218, *Standard Test Method for Determining Forming Limit Curves*, p.5, American Society for Testing and Materials, West Conshohocken, USA (2002).
21. M. Hajian and A. Assempour, *Int. J. Adv. Manuf. Technol.* **76**, 1757 (2015).
22. *LS-DYNA Keyword User's Manual Version 971*, Vol 1, 424 (MAT), Livermore software technology corporation, California (2007).
23. K. H. Lo, D. Zeng, and C. T. Kwok, *Mater. Sci. Eng. A* **528**, 1003 (2011).
24. A. Das and S. Tarafder, *Int. J. Plast.* **25**, 2222 (2009).
25. W. J. Dan, W. G. Zhang, S. H. Li, and Z. Q. Lin, *Comput. Mater. Sci.* **40**, 101 (2007).
26. R. Zaera, J. A.R. Martinez, A. Casado, J. F. Saez, A. Rusinek, and R. Pesci, *Int. J. Plast.* **29**, 77 (2012).
27. N. Li, Y. D. Wang, W. J. Liu, Z. N. An, J. P. Liu, R. Su, J. Li, and P. K. Liaw, *Acta Mater.* **64**, 12 (2014).
28. H. K. Yeddu, T. Lookman, and A. Saxena, *Acta Mater.* **61**, 6972 (2013).